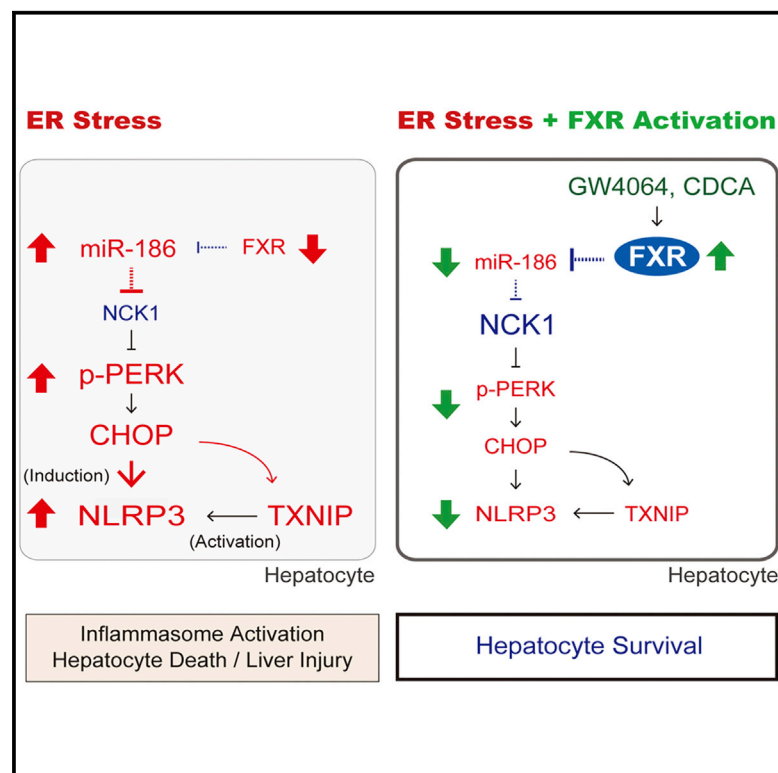


FXR Inhibits Endoplasmic Reticulum Stress-Induced NLRP3 Inflammasome in Hepatocytes and Ameliorates Liver Injury

Graphical Abstract



Authors

Chang Yeob Han, Hyun Soo Rho, Ayoung Kim, ..., Jong Won Kim, Bumseok Kim, Sang Geon Kim

Correspondence

sgk@snu.ac.kr

In Brief

Han et al. demonstrate that FXR inhibits ER stress-induced NLRP3 inflammasome activation in hepatocytes. FXR activation ameliorates ER stress-dependent hepatocyte death and liver injury. These findings provide insight into ER stress-mediated inflammasome activation and liver disease progression.

Highlights

- FXR inhibits ER stress-induced NLRP3 inflammasome activation in hepatocytes
- FXR attenuates ER stress-induced hepatocyte death and liver injury
- FXR inhibits NLRP3 and TXNIP expression through the PERK-CHOP pathway
- miR-186 and its potential target, Nck1, are involved in the ER stress inhibition by FXR



FXR Inhibits Endoplasmic Reticulum Stress-Induced NLRP3 Inflammasome in Hepatocytes and Ameliorates Liver Injury

Chang Yeob Han,^{1,2,6} Hyun Soo Rho,^{1,6} Ayoung Kim,¹ Tae Hyun Kim,¹ Kiseok Jang,³ Dae Won Jun,⁴ Jong Won Kim,⁵ Bumseok Kim,⁵ and Sang Geon Kim^{1,7,*}

¹College of Pharmacy and Research Institute of Pharmaceutical Sciences, Seoul National University, Seoul 08826, Korea

²Department of Pharmacology, School of Medicine, Wonkwang University, Iksan, Jeonbuk 54538, Korea

³Department of Pathology, Hanyang University School of Medicine, Seoul 04763, Korea

⁴Internal Medicine, Hanyang University School of Medicine, Seoul 04763, Korea

⁵Biosafety Research Institute and Laboratory of Pathology, College of Veterinary Medicine, Chonbuk National University, Iksan, Jeonbuk 54596, Korea

⁶These authors contributed equally

⁷Lead Contact

*Correspondence: sgk@snu.ac.kr

<https://doi.org/10.1016/j.celrep.2018.07.068>

SUMMARY

Endoplasmic reticulum (ER) stress is associated with liver injury and fibrosis, and yet the hepatic factors that regulate ER stress-mediated inflammasome activation remain unknown. Here, we report that farnesoid X receptor (FXR) activation inhibits ER stress-induced NACHT, LRR, and PYD domains-containing protein 3 (NLRP3) inflammasome in hepatocytes. In patients with hepatitis B virus (HBV)-associated hepatic failure or non-alcoholic fatty liver disease, and in mice with liver injury, FXR levels in the liver inversely correlated with the extent of NLRP3 inflammasome activation. *Fxr* deficiency in mice augmented the ability of ER stress to induce NLRP3 and thioredoxin-interacting protein (TXNIP), whereas FXR ligand activation prevented it, ameliorating liver injury. FXR attenuates CCAAT-enhancer-binding protein homologous protein (CHOP)-dependent NLRP3 overexpression by inhibiting ER stress-mediated protein kinase RNA-like endoplasmic reticulum kinase (PERK) activation. Our findings implicate miR-186 and its target, non-catalytic region of tyrosine kinase adaptor protein 1 (NCK1), in mediating the inhibition of ER stress by FXR. This study provides the insights on how FXR regulation of ER stress ameliorates hepatocyte death and liver injury and on the molecular basis of NLRP3 inflammasome activation.

INTRODUCTION

Hepatocyte injury initiates and facilitates inflammation in the course of liver disease progression. Thus, understanding the regulatory basis for sensing and responding to damage-associ-

ated inflammatory processes in the liver's parenchymal cells is a primary issue in liver pathophysiology. The inflammasome is a multiprotein complex that senses cellular danger signals, and its activation leads to interleukin (IL)-1 β production (Guo et al., 2015). Emerging evidence suggests that the NACHT, LRR, and PYD domains-containing protein 3 (NLRP3) inflammasome in hepatocytes plays a role in the pathogenesis of liver diseases (Szabo and Csak, 2012; Szabo and Petrasek, 2015). In particular, saturated fatty acid activates the NLRP3 inflammasome and sensitizes hepatocytes to endotoxin response, leading to non-alcoholic steatohepatitis (NASH) (Csak et al., 2011). Uric acid also induces fat accumulation in the liver and insulin resistance through the NLRP3 inflammasome (Wan et al., 2016). Thus, NLRP3 has an impact on hepatocyte death, inflammation, and potentially on the progression of liver fibrosis, as shown in an animal study (Wree et al., 2014). Nevertheless, the endogenous molecules and pathways that regulate these NLRP3-mediated events are largely unknown.

Multiple disturbances that cause the accumulation of misfolded or unfolded proteins in the endoplasmic reticulum (ER) trigger the ER stress response (i.e., the unfolded protein response [UPR]; Hetz, 2012). Chronic or irremediable ER stress then induces cellular dysfunction and eventually leads to cell death, which is closely associated with hepatic inflammation (Dara et al., 2011; Malhi and Kaufman, 2011). NLRP3 is a member of the inflammasome family that is activated by diverse pathological stimuli, including extracellular ATP, cholesterol crystals, and reactive oxygen species, as well as microbial pathogens (Szabo and Csak, 2012; Szabo and Petrasek, 2015), suggestive of its critical role in sterile inflammation. It has also been proposed that ER stress is linked to the NLRP3 inflammasome in pancreatic beta cells (Lerner et al., 2012; Osowski et al., 2012). ER stress also induces inflammasome activation in hepatocytes, potentially causing liver injury (Lebeaupin et al., 2015). However, the hepatic regulator that acts to ameliorate ER stress and the inflammasome remains unknown.

Farnesoid X receptor (FXR) (NR1H4) serves as a ligand-mediated transcription factor that controls the expression of various



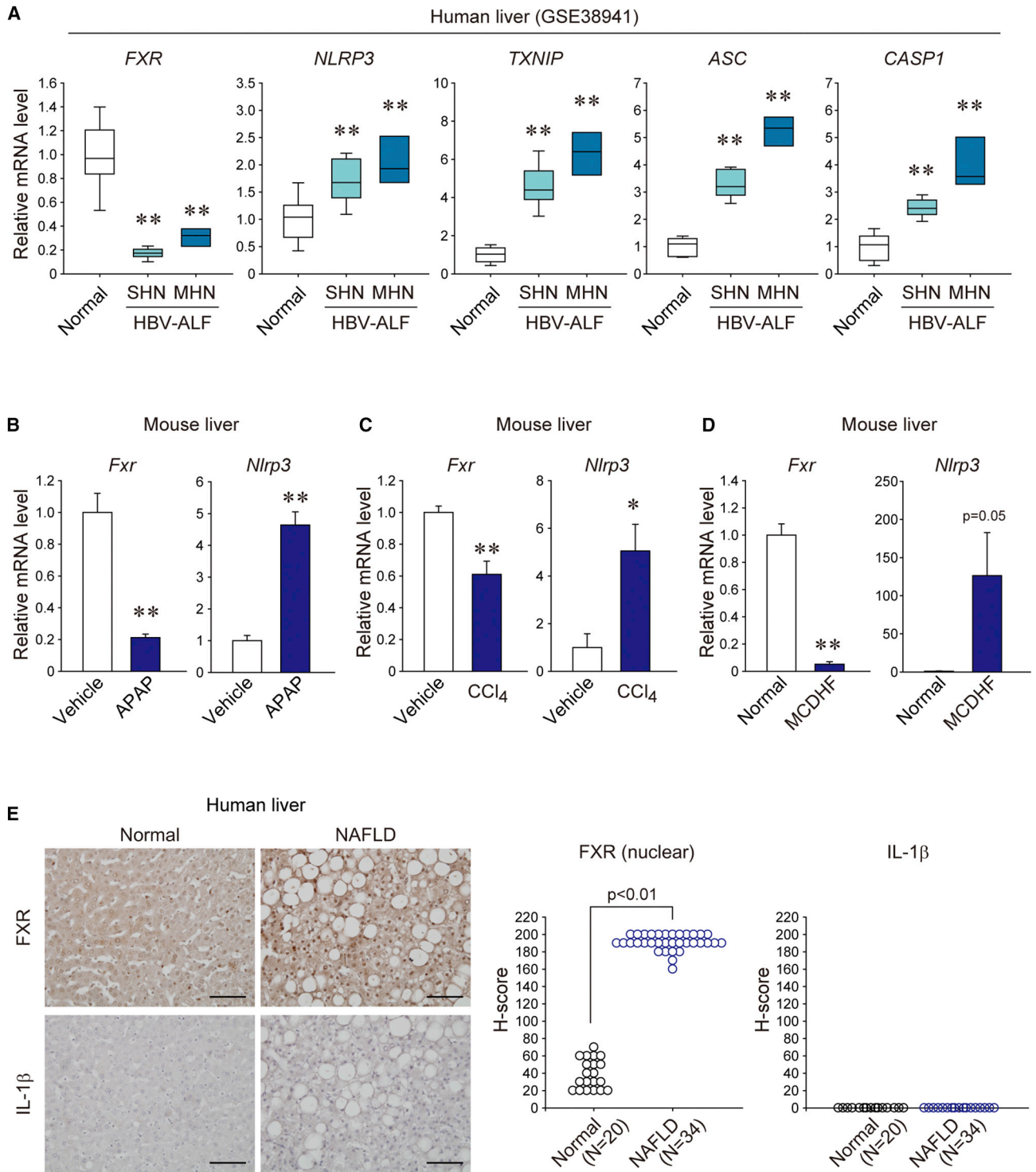


Figure 1. FXR Levels Inversely Correlate with NLRP3 Inflammasome Marker Levels in Liver Disease Conditions

(A) *FXR* and *NLRP3* inflammasome gene transcript levels in patients with acute liver failure. Hepatic transcript levels were analyzed in healthy individuals (normal) or in patients with HBV-associated acute liver failure (GSE38941). MHN, massive hepatic necrosis; SHN, submassive hepatic necrosis. Data are shown as box and whisker plot. Box, interquartile range (IQR); whiskers, 5–95 percentiles; horizontal line within box, median. Statistical significance of the differences between healthy individuals and patients with liver failure (** $p < 0.01$) was determined (N = 10 samples from 10 individual normal subjects; N = 8 samples from 2 patients with SHN-ALF; N = 9 samples from 2 patients with MHN-ALF; as described in GSE38941 database).

(legend continued on next page)

genes involved in bile acid, lipid, and glucose metabolism (Calkin and Tontonoz, 2012; Teodoro et al., 2011). FXR plays a role in the maintenance of liver homeostasis and is also important for mitochondrial function and cellular integrity (Lee et al., 2012; Wang et al., 2008). The ligand-mediated activation of FXR in the liver has beneficial effects against metabolic disorders. Indeed, FXR ligands have been tested in clinical trials for the treatment of non-alcoholic fatty liver disease (NAFLD), diabetes, and cholestasis (Adorini et al., 2012; Beuers et al., 2015; Carr and Reid, 2015). However, the anti-inflammatory effect exerted by FXR in hepatocytes, in particular, in the context of liver protection against ER stress-mediated injury needs to be established.

In view of the lack of an understanding about NLRP3 regulators and of the potential anti-inflammatory action of FXR in hepatocytes, this study investigated the inhibitory role of FXR in NLRP3 inflammasome activation in response to ER stress. First, we used bioinformatic approaches and analyzed human liver samples to investigate the action of FXR on the target of interest and performed loss- or gain-of-function experiments in animal and cell models. Our results demonstrate that FXR levels in the liver inversely correlate with those of inflammasome gene expression in patients with hepatitis B virus (HBV)-associated liver failure or with NAFLD and that ligand-mediated activation of FXR prevents ER stress from activating the NLRP3 inflammasome in hepatocytes. In addition, we found that FXR inhibits the protein kinase RNA-like endoplasmic reticulum kinase (PERK)-CCAAT-enhancer-binding protein homologous protein (CHOP) pathway, inhibiting the priming and activation steps of the NLRP3 inflammasome. We further propose, based on our findings from *in vivo* and *in vitro* ER stress models, that miR-186 and its potential target, non-catalytic region of tyrosine kinase adaptor protein 1 (NCK1), mediates the inhibition of ER stress by FXR.

RESULTS

Hepatic FXR Levels Inversely Correlate with NLRP3 Inflammasome Marker Levels

To investigate the functional impact of FXR on inflammasome activation in different liver diseases, we analyzed *FXR* and *NLRP3* transcript levels in healthy (normal) individuals and in patients with HBV-associated acute liver failure, using data from the publicly accessible human GEO database (GEO: GSE38941; Nisim et al., 2012). Hepatic *FXR* transcript levels were decreased in patients with HBV-associated acute liver failure (HBV-ALF), relative to *FXR* transcript levels in normal controls (Figure 1A). Intriguingly, the levels of *NLRP3* and other inflammasome-associated gene transcripts (i.e., thioredoxin-interacting protein [*TXNIP*], apoptosis-associated speck-like caspase activation and recruitment domain (CARD)-containing protein [ASC], and caspase-1 [*CASP1*]) increased markedly as hepatic necrosis became

severe, although *FXR* levels decreased (Figure 1A). In our recent study, ER stress marker levels were enhanced in patients with liver injury (Han et al., 2016). To confirm inflammasome activation in an animal model of liver injury, we examined liver samples from mice treated with the drug acetaminophen (APAP), which induces ER stress and liver damage (Han et al., 2016). In these liver samples, *Fxr* transcript levels were decreased, and *Nlrp3* levels were increased relative to untreated controls (Figure 1B). Similar results were obtained from liver samples from mice treated with carbon tetrachloride (CCl_4) (Figure 1C).

NASH can be induced in mice by feeding them a methionine- and choline-deficient high-fat (MCDHF) diet (Park et al., 2016). To confirm the inverse relationship between FXR and NLRP3, we assayed *Fxr* and *Nlrp3* levels in the physiologically relevant NASH mouse model and observed a profound decrease of *Fxr* in the livers of these mice, together with increased levels of *Nlrp3* (Figure 1D). We also investigated FXR expression in the livers of patients with NAFLD and found it to be higher than in normal individuals, as shown by immunohistochemical assays (Figure 1E, left). Quantification using H scoring verified this outcome (Figure 1E, right). IL-1 β is the ultimate measure of inflammasome activation. Consistently, IL-1 β levels were not changed in the liver samples of patients with NAFLD (Figure 1E, left and right). These results show that FXR levels in the liver inversely correlate with the extent of NLRP3 inflammasome activation in different liver diseases, raising the hypothesis that FXR inhibits ER stress-induced NLRP3 inflammasome activation.

ER Stress Induces NLRP3 and TXNIP in Hepatocytes in Association with FXR Repression

To assess the relationship between FXR and the NLRP3 inflammasome under the condition of ER stress, we used tunicamycin (Tm) as an ER stress inducer in animal or cell models. Mice treated with Tm showed a marked decrease in hepatic FXR levels (Figure 2A). In contrast, NLRP3 and TXNIP levels were substantially increased with minimal changes observed to ASC levels (Figure 2A), highlighting NLRP3 and TXNIP as being appropriate markers of inflammasome activation to use in subsequent experiments. Following Tm treatment, cleaved CASP1 levels were also consistently enhanced, confirming that ER stress had activated the inflammasome in the liver (Figure 2A). Our results showed that ER stress inhibits FXR expression in the liver, which may facilitate NLRP3 inflammasome activation. To address whether ER stress has a direct effect on hepatocytes, we utilized primary hepatocytes and the hepatocyte-derived AML12 cell line and obtained similar results (Figure 2B). Thus, it is highly likely that ER stress activates the NLRP3 inflammasome in hepatocytes in association with decreased FXR levels. Increased levels of IL-1 β in the livers of Tm-treated mice (as assayed by immunohistochemistry; Figure 2C) and in

(B–D) *Fxr* and *Nlrp3* transcript levels in mouse liver. For (B), mice were injected with vehicle or APAP (500 mg/kg body weight, i.p., 6 hr; N = 5 or 6 for each treatment). For (C), mice were treated with vehicle or CCl_4 (0.6 mL/kg, i.p., twice a week) for 6 weeks (N = 4 or 5 each treatment). For (D), mice were fed a control diet or a methionine- and choline-deficient high-fat (MCDHF) diet for 6 weeks (N = 6 for each diet). Data represent the mean \pm SEM. Statistical significance of the differences between each treatment group and vehicle or control diet (* $p < 0.05$; ** $p < 0.01$) was determined.

(E) Immunohistochemistry for nuclear FXR and IL-1 β in the liver of patients with NAFLD. FXR and IL-1 β levels were semi-quantified based on staining intensity and percentage of positive cells, and H scores were assigned (N = 20 for normal; N = 34 for NAFLD). The extent of expression was calculated using staining-positive cells per ten high-power fields (scale bars, 50 μm).

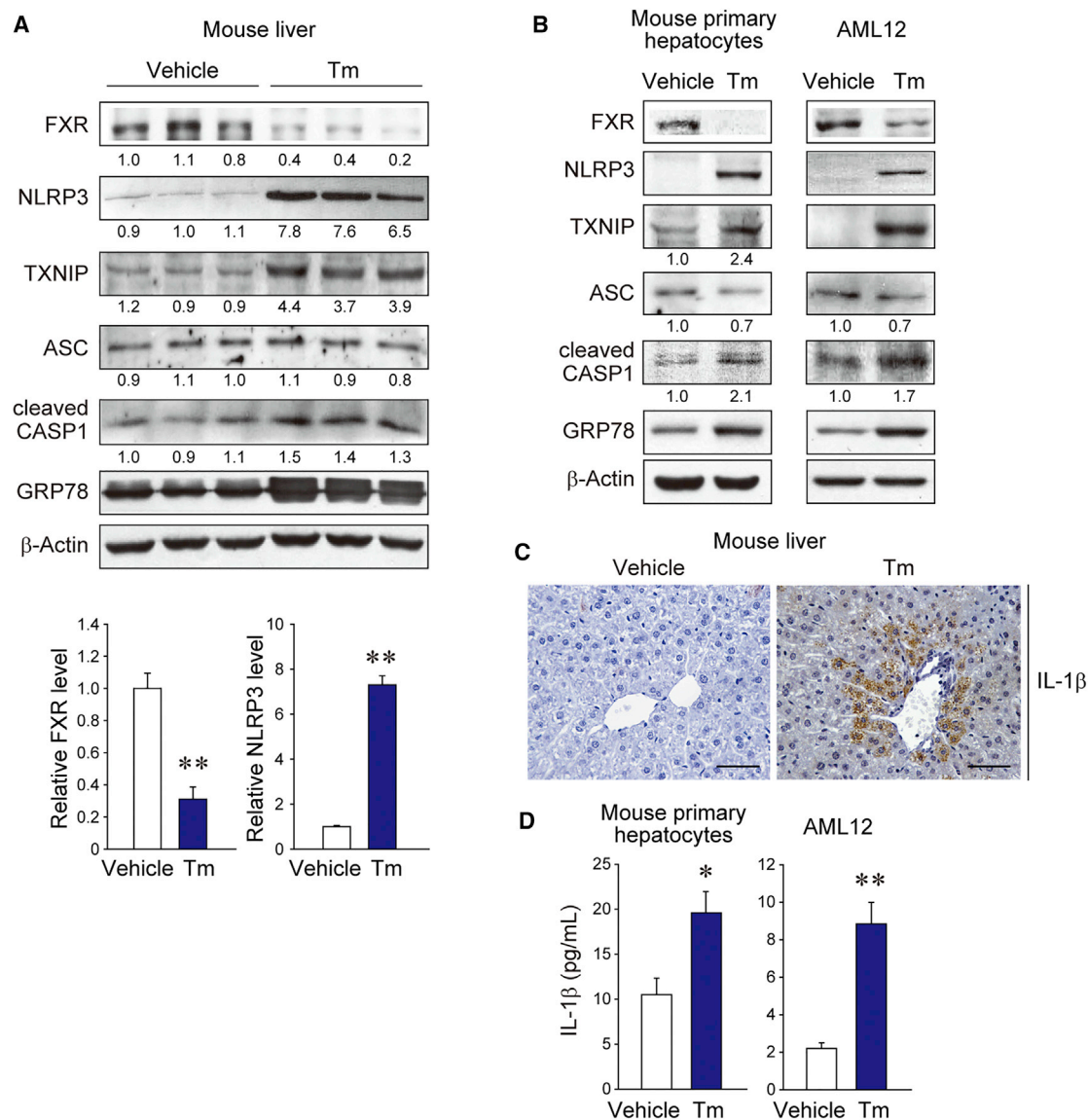


Figure 2. ER Stress Represses FXR in Hepatocytes for NLRP3 Inflammasome Activation

(A and B) Immunoblots for FXR and NLRP3 inflammasome markers. For (A), assays were done 3 days after treatment of mice with a single intraperitoneal dose of vehicle or tunicamycin (Tm) (2 mg/kg body weight). Data represent the mean \pm SEM (N = 3 each treatment). For (B), mouse primary hepatocytes or AML12 cells were treated with vehicle or 1 μ M Tm for 24 hr. Relative protein levels were assessed by scanning densitometry of the immunoblots. Values indicate the relative protein levels to β -actin.

(C) Immunohistochemistry for IL-1 β in the liver (scale bars, 50 μ m).

(D) ELISA for mature IL-1 β . Assays were done on the media from mouse primary hepatocytes or AML12 cells that had been treated with vehicle or 1 μ M Tm for 24 hr. Data represent the mean \pm SEM (N = 4 or 5 each).

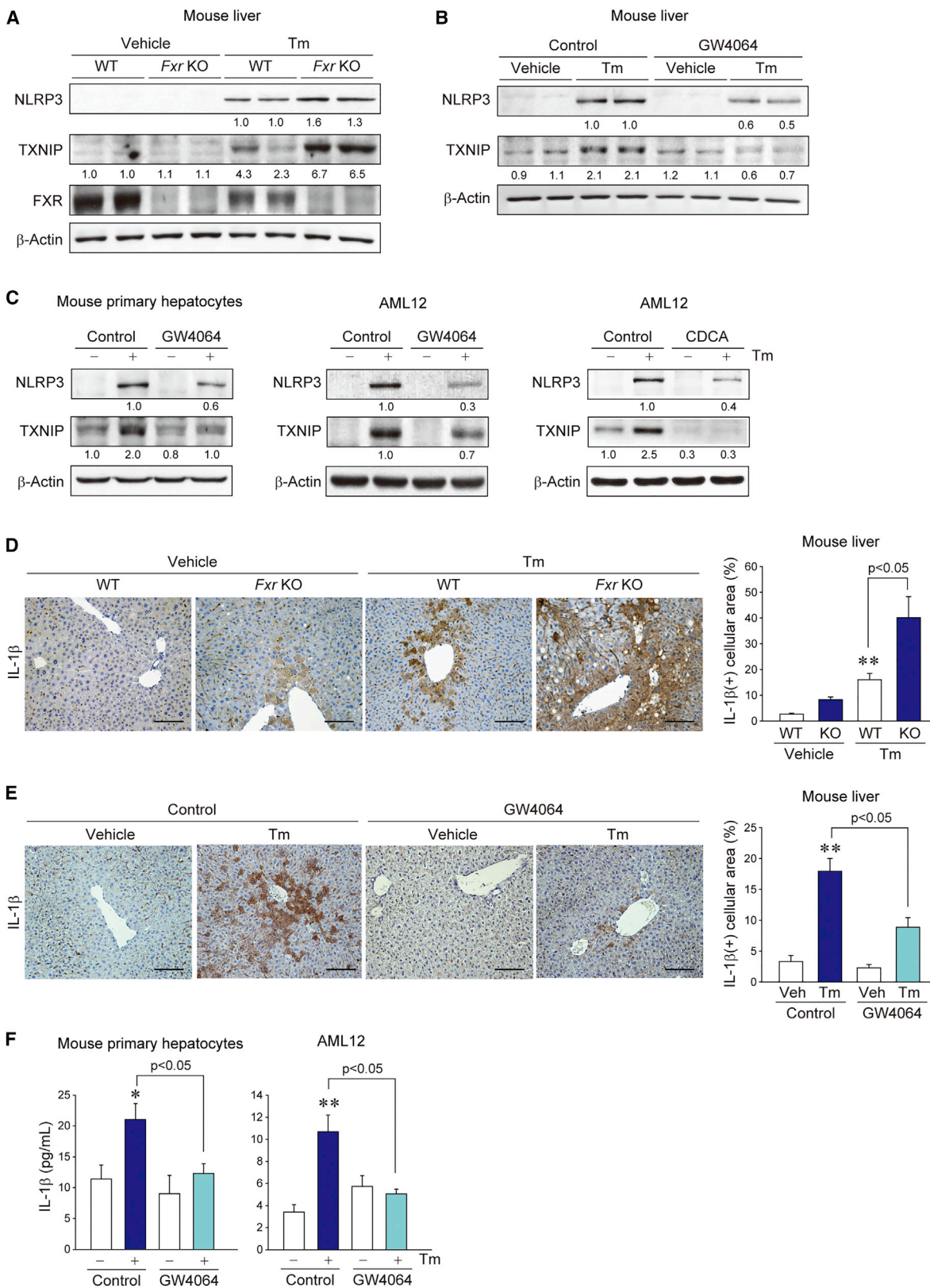
In (A) and (D), *p < 0.05, **p < 0.01.

Tm-treated mouse primary hepatocytes and AML12 cells (as assayed by ELISA; Figure 2D) corroborated that ER stress induces inflammasome activation.

Fxr Ablation Worsens ER Stress-Induced Inflammasome Activation and Hepatocyte Injury

To determine the effect of modulating FXR activities on ER stress-induced NLRP3 inflammasome activation, we next per-

formed *Fxr* loss- or gain-of-function experiments in mice. *Fxr* gene knockout (KO) in mice did not on its own increase the levels of inflammasome markers in the liver. Interestingly, however, *Fxr* KO enhanced the inducing effect of Tm on NLRP3 and TXNIP levels in the mouse livers (Figure 3A). Consistently, the treatment of wild-type mice with GW4064, an FXR agonist (Maloney et al., 2000), attenuated the induction of NLRP3 and TXNIP under ER stress condition (Figure 3B). Similar results were obtained using



(legend on next page)

mouse primary hepatocytes or AML12 cells (Figure 3C, left and middle). FXR activation by GW4064 was validated using FXR response-element reporter activity (Figure S1). The ability of FXR to inhibit NLRP3 and TXNIP was also experimentally verified in AML12 cells by using chenodeoxycholic acid (CDCA), a representative endogenous ligand of FXR (Figure 3C, right). The inhibition of ER stress-induced inflammasome activation by FXR was also corroborated by assaying IL-1 β levels in the livers of wild-type and *Fxr* KO mice (via immunostaining; Figures 3D and 3E) and in hepatocyte cell models (via ELISA; Figure 3F).

Inflammasome activation has been shown to magnify hepatocyte injury and inflammation in the liver (Szabo and Csak, 2012; Wree et al., 2014). To evaluate the functional outcome of inflammasome activation in hepatocytes, we monitored the blood biochemistry and liver histopathology of wild-type and *Fxr* KO mice. Loss of FXR markedly potentiated ER stress-mediated increases in alanine transaminase, aspartate transaminase, and lactate dehydrogenase activities in the serum (Figure 4A), whereas the ligand-mediated activation of FXR had the opposite effect (Figure 4B). The modulating effects of FXR on ER stress-induced hepatocyte injury were verified by the histopathological examination of liver tissue, which showed that hepatocytes from *Fxr* KO mice exhibit ballooning, degeneration, and necrosis upon ER stress challenge (Figure 4C). Consistently, GW4064 treatment exerted the opposite effect (Figure 4D). Similar outcomes were obtained in the analyses of apoptosis by terminal transferase-mediated dUTP nick-end labeling (TUNEL) staining and from the quantification of TUNEL-positive cell number (Figures 4E and 4F). Thus, our results demonstrate that the loss of FXR facilitates the activation of the NLRP3 inflammasome and hepatocyte injury by ER stress in the liver and that this activation can be overcome by the ligand-mediated activation of FXR.

FXR Inhibits NLRP3 and TXNIP through the PERK-CHOP Pathway

To identify the FXR regulatory pathway in the ER stress-induced activation of the NLRP3 inflammasome, we examined representative molecular markers and performed UPR pathway analyses using small interfering RNA (siRNA) transfection techniques. *Fxr* KO mice displayed increased p-PERK and CHOP levels upon ER stress, which paralleled the levels of glucose-regulated protein 78 (GRP78) (Figure 5A, left). The spliced form of X-box binding protein-1 (XBP1), a transcription factor that lies downstream of the inositol-requiring enzyme-1 (IRE1), was unaffected by the loss of FXR (Figure 5A, left). Consistently, GW4064 treatment attenuated the effect of Tm on p-PERK and CHOP levels in mice (Figure 5A, middle). The ability of FXR to ameliorate the

ER stress-mediated activation of PERK and CHOP was also confirmed using hepatocyte cell models (Figure 5A, right). GW4064 treatment did not alter the Tm-induced mRNA splicing of *Xbp1* in our experimental conditions (Figure S2A).

The transfection of AML12 cells with *Perk* siRNA prevented ER stress, as induced by Tm, from increasing NLRP3, TXNIP, and CHOP levels (Figure 5B). The siRNA-mediated knockdown of *Irf1* decreased TXNIP, but not NLRP3 (Figure 5C), although the knockdown of *Atf6* had no effect on NLRP3 and TXNIP levels (Figure 5D). Overall, our results show that the induction of NLRP3 and TXNIP by ER stress is differentially regulated by UPR pathways, indicating that the PERK pathway is enhanced by the loss of FXR and facilitates the activation of the NLRP3 inflammasome in hepatocytes.

Because CHOP is a major transcriptional regulator of the genes downstream of PERK that are associated with cell death, we investigated whether CHOP plays a role in the induction of NLRP3 or TXNIP. The siRNA-mediated knockdown of *Chop* reduced the effect of Tm on NLRP3 and TXNIP expression (Figure 5E). The likelihood that CHOP transcriptionally regulates NLRP3 was strengthened by the results of the chromatin immunoprecipitation (ChIP) assays, which identified putative CHOP DNA-binding sites in the promoter region of the human *NLRP3* gene (Figure 5F). Consistently, *Perk* overexpression in AML12 cells significantly enhanced *Nlrp3* transcription (Figure 5G). The role of PERK in NLRP3 inflammasome activation in hepatocytes was further verified by the reduction in IL-1 β production in AML12 cells, in which *Perk* was knocked down (Figure 5H). These results indicate that PERK activation contributes to the activation of the NLRP3 inflammasome by ER stress in hepatocytes through the CHOP-dependent induction of NLRP3.

TXNIP plays a role in the NLRP3 activation step (Osowski et al., 2012; Zhou et al., 2010). Given the regulatory effect of PERK/CHOP on TXNIP, as well as on NLRP3, we additionally examined the modulating effect of TXNIP on NLRP3 in hepatocytes and found that *Txnip* knockdown did not change NLRP3 or CHOP levels (Figure S2B), indicating that the ER stress-mediated induction of NLRP3 might be independent of TXNIP. Overall, our results provide evidence that FXR inhibits PERK under the condition of ER stress and that PERK regulates the CHOP-mediated induction of NLRP3 and TXNIP overexpression.

NCK1 Is Involved in the FXR Inhibition of the ER Stress-Induced NLRP3 Inflammasome

The activity of PERK is negatively regulated by NCK1 (Yamani et al., 2014). To understand the molecular basis that underlies the regulation of PERK and the NLRP3 inflammasome by FXR,

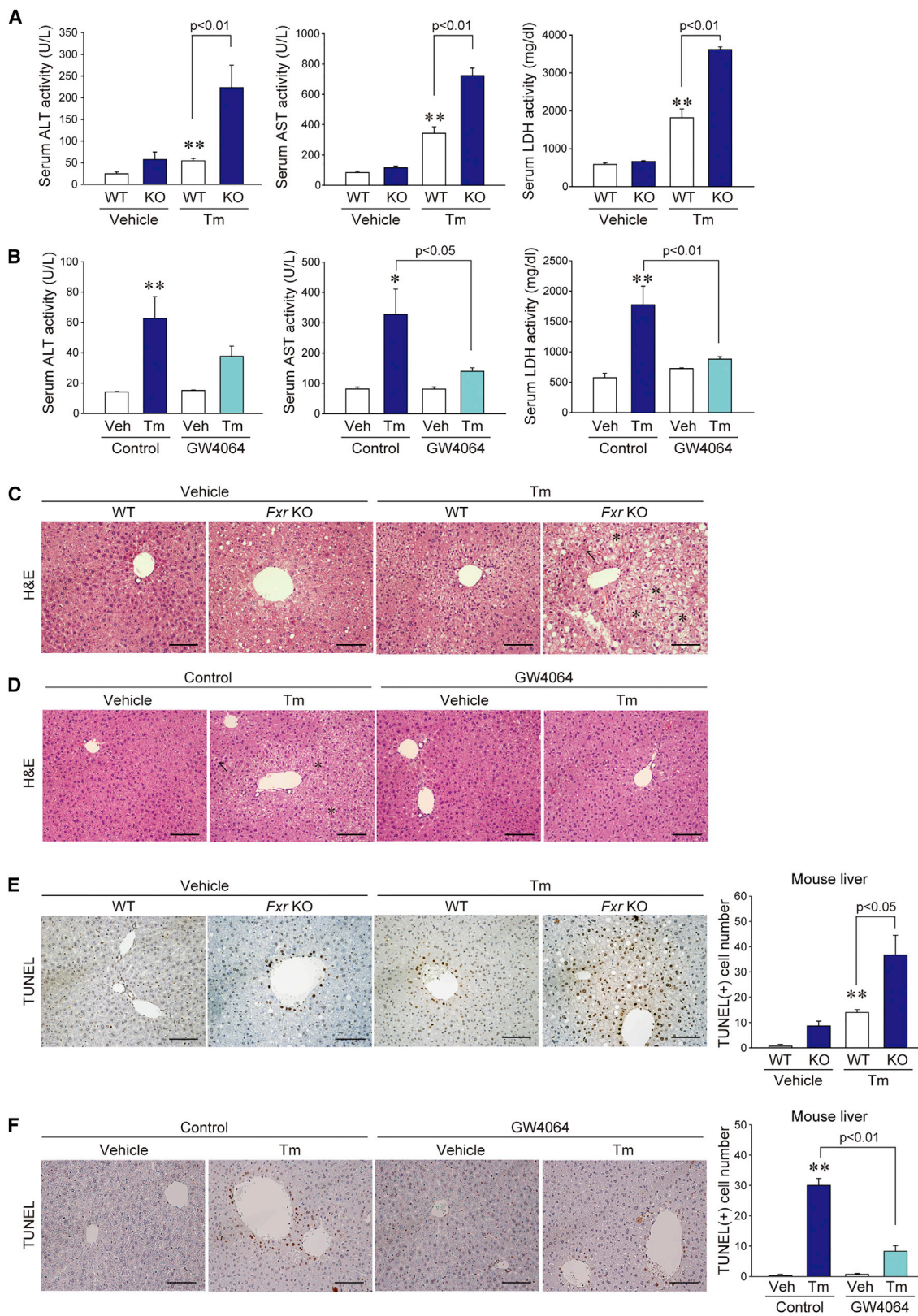
Figure 3. FXR Inhibits NLRP3 Inflammasome Activation by ER Stress

(A and B) Immunoblots for NLRP3 and TXNIP in mouse liver. Assays were done 2 days after treatment with a single intraperitoneal dose of vehicle or Tm (N = 4 or 6 for each treatment; A) or 3 days after intraperitoneal injection with Tm following GW4064 (30 mg/kg) treatment (N = 5 or 7 for each treatment; B). Treatment schedule details are provided in the Experimental Procedures section. Relative protein levels were presented as in Figures 2A and 2B.

(C) Immunoblots for NLRP3 and TXNIP in hepatocytes. Mouse primary hepatocytes were pre-treated with GW4064 (1 μ M; 1 hr) and continuously incubated with Tm for 24 hr (left). AML12 cells were similarly treated with Tm after treatment with GW4064 or CDCA (100 μ M; 1 hr; middle and right).

(D and E) Immunohistochemistry for IL-1 β on mouse liver sections from wild-type (WT) and *Fxr* KO mice (D), controls, or treated with Tm and/or GW4064 (E) (scale bars, 100 μ m). Data represent the mean \pm SEM (N = 3 each). Statistical significance of differences between each treatment and control group (**p < 0.01) was determined.

(F) ELISA for mature IL-1 β . Assays were done on the media prepared from the cells treated as in (C). Data represent the mean \pm SEM (N = 3 or 5 each). See also Figure S1.



(legend on next page)

we hypothesized that NCK1 mediates the inhibition of ER stress by FXR. In support of this hypothesis, we found that hepatic NCK1 levels were significantly lower in *Fxr* KO mice than in wild-type mice (Figure 6A). In addition, in hepatocyte cell models, we observed that ER stress decreased the levels of NCK1 and that this effect was significantly reversed by FXR ligand treatment (Figure 6B), indicating a regulatory effect of FXR on NCK1. GW4064 treatment alone did not notably change NCK1 levels in these experimental conditions. We then examined the effect that modulating NCK1 had on the inhibitory effect of FXR on our targets of interest and found that *Nck1* knockdown significantly attenuated the effects of GW4064 on NLRP3, TXNIP, and CHOP under ER stress conditions (Figure 6C). In view of the association of inflammasome activation with cell death, we assessed the viability of AML12 cells under similar experimental conditions. GW4064 treatment increased the viability of these cells under conditions of ER stress; however, this protection was significantly reduced following the siRNA-mediated knockdown of *Nck1* (Figure 6D). These results indicate that NCK1 might be associated with the inhibitory effect of FXR on ER stress-induced NLRP3 inflammasome activation and cell death.

miR-186 Regulates the ER Stress-Induced NLRP3 Inflammasome

In a continuing effort to find the molecule(s) that regulates NCK1, we examined whether FXR binding sites exist in the promoter region of the *Nck1* gene using PROMO search analysis and found no such sites. We therefore tested the possibility that NCK1 undergoes post-transcriptional regulation. One major form of post-transcriptional regulation is mediated by microRNAs. Using the database “miRanda (microrna.org)”, we selected the top five microRNAs (miRNAs) that have the potential to bind to the 3' UTR of *Nck1* mRNA. Of these five miRNAs, miR-186 was found to be increased in the livers of *Fxr* KO mice (Figure 7A) and in response to ER stress (Figure 7B). Moreover, this ER stress-induced increase in miR-186 levels was abrogated by the ligand-mediated activation of FXR (Figure 7B). As with NCK1 (Figure 6B), GW4064 treatment alone had no significant effect on miR-186 levels (Figure 7B). To understand the role of miR-186 in NCK1 inhibition, the effect that miR-186 modulation has on NCK1 was assessed using a miR-186 mimic and inhibitor. When AML12 cells were transfected with a miR-186 mimic, NCK1 levels decreased, whereas NCK1 levels increased following transfection with a miR-186 antisense oligonucleotide (ASO) (Figure 7C). The inhibitory effect of miR-186 on NCK1 was further supported by assaying the effects of the miR-186 mimic and ASO in a *Nck1* 3' UTR reporter assay (Figure 7D). These results suggest that FXR might contribute to the regulation of NCK1 by miR-186 in hepatocytes under conditions of ER stress.

We additionally examined the role of the identified molecules (i.e., miR-186/NCK1/PERK) in the induction of the NLRP3 inflammasome by ER stress in association with FXR. In time course studies, miR-186 levels increased maximally in AML12 cells 1 hr after Tm treatment and declined thereafter (Figure 7E, left), whereas *Chop* mRNA levels began to increase 6 hr after Tm treatment and peaked at 12 hr (Figure 7E, middle). *Nlrp3* mRNA increased to the greatest extent 24 hr after Tm treatment (Figure 7E, right). Thus, the increase in miR-186 preceded the changes in CHOP signaling, which then led to NLRP3 induction. miR-186 mimic transfection attenuated the effects of GW4064 on NLRP3, TXNIP, and CHOP under ER stress conditions (Figure 7F). Consistently, miR-186 ASO also had inhibitory effects on the levels of NLRP3, TXNIP, p-PERK, p-eukaryotic initiation factor 2 α (eIF2 α) (another NCK1 target; Latreille and Larose, 2006), and CHOP upon ER stress challenge, which was reversed by *Nck1* knockdown (Figure 7G). Thus, the molecules identified in this study are functionally involved in the regulation of the ER stress-dependent NLRP3 inflammasome pathway. Together, our results show that the loss of FXR elicited by ER stress contributes to the PERK-mediated activation of the NLRP3 inflammasome, probably through miR-186/NCK1 dysregulation, and that this event can be overcome by FXR activation.

DISCUSSION

The inflammasome consists of the sensor molecule nucleotide oligomerization domain (NOD)-like receptors (NLRs), the adaptor protein ASC, and the effector molecule CASP1 (Guo et al., 2015). Among the different types of inflammasome, the NLRP3 inflammasome requires a priming step because the basal expression of NLRP3 is insufficient; its upregulation is thus essential for inflammasome activation (Guo et al., 2015; Szabo and Csak, 2012). NLRP3 activation is mediated by two major steps: the expression of inflammasome components (signal 1) and their functional activation (signal 2; Szabo and Csak, 2012). Here, we report a functional role for FXR in the regulation of the NLRP3 inflammasome in hepatocytes. Our analysis of the GEO database showed that FXR is downregulated in patients with hepatic necrosis, whereas NLRP3 is upregulated, revealing the existence of an inverse relationship between FXR and the NLRP3 inflammasome. This inverse relationship was confirmed in animal models of induced liver injury (via APAP or CCl₄ treatment or the MCDHF diet), showing that FXR is downregulated with NLRP3 inflammasome activation in different liver disease conditions.

Our results from *Fxr* KO mice and from their treatment with an FXR agonist revealed that FXR can suppress the NLRP3 inflammasome when it is activated by ER stress in hepatocytes. Consistently, the data also showed that FXR activation inhibits

Figure 4. FXR Activation Protects Hepatocytes from ER Stress-Induced Injury

(A and B) Serum alanine transaminase (ALT), aspartate transaminase (AST), and lactate dehydrogenase (LDH) activities in mice treated as in Figures 3A and 3B. Data represent the mean \pm SEM (N = 4–6). Statistical significance of differences between each treatment and control group (*p < 0.05; **p < 0.01) was determined. (C and D) H&E staining of liver sections from wild-type (WT) and *Fxr* KO mice (C), controls, or treated with Tm and/or GW4064 (D). Mice were treated as in Figures 3A and 3B (scale bars, 100 μ m). Asterisks indicate ballooning degeneration of hepatocytes, whereas arrows represent hepatic necrosis. (E and F) TUNEL staining of the liver sections from wild-type (WT) and *Fxr* KO mice (E), controls, or treated with Tm or GW4064 (F). Mice were treated as in Figures 3A and 3B (scale bars, 100 μ m). Data represent the mean \pm SEM (N = 3 each). **p < 0.01.

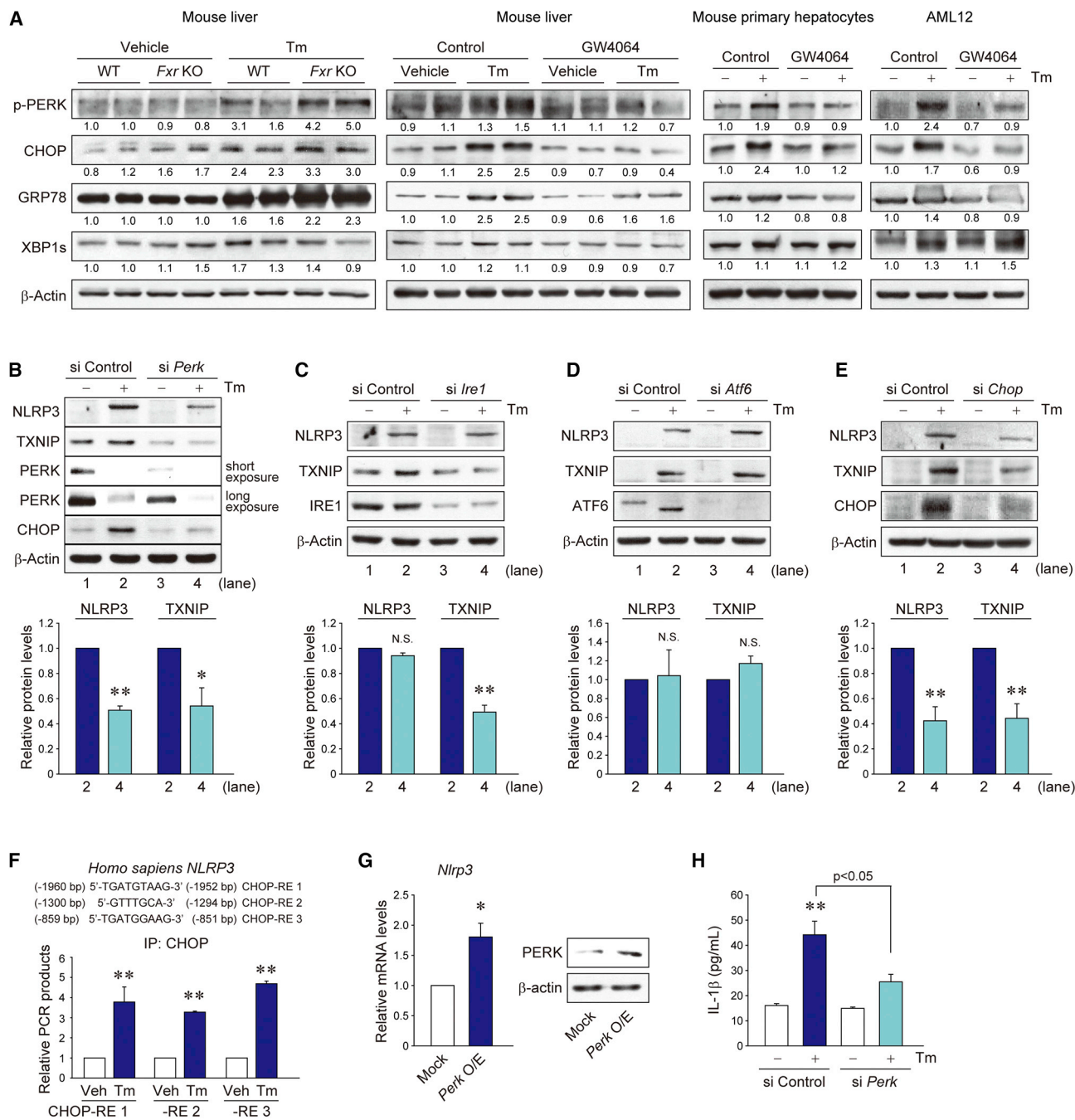


Figure 5. FXR Inhibits PERK-CHOP Pathway for Regulation of NLRP3 and TXNIP

(A) Immunoblots for ER stress markers in mouse liver or hepatocytes. Animals or cells were treated as in Figure 3C.

(B–D) Immunoblots for NLRP3 and TXNIP after knockdown of each UPR pathway. AML12 cells were treated with vehicle or Tm (1 μ g/mL for 24 hr) after transfection with control siRNA or each specific siRNA against *Perk* (B), *Ire1* (C), or *Atf6* (D) for 48 hr. Immunoblots confirmed the knockdown effects. Data represent the mean \pm SEM of three separate experiments. Statistical significance of the differences between Tm+each target siRNA and Tm+siControl (* p < 0.05; ** p < 0.01) was determined (N.S., not significant).

(E) Immunoblots for NLRP3 and TXNIP after *Chop* knockdown. AML12 cells were treated as described in (B)–(D) after siRNA knockdown of *Chop*. Data represent the mean \pm SEM of three separate experiments.

(F) ChIP assays for CHOP DNA binding. ChIP assays were performed on the lysates of HepG2 cells treated with Tm (5 μ g/mL; 12 hr). DNA-protein complexes were precipitated with anti-CHOP antibody and were subjected to PCR amplifications using the flanking primers for the CHOP-response elements (CHOP-REs). One-tenth of cross-linked lysates served as the input control. Data represent the mean \pm SEM (N = 3 or 4 each).

(legend continued on next page)

NLRP3 and TXNIP, as well as ER stress-induced IL-1 β secretion from the NLRP3 inflammasome. The concept that FXR negatively regulates the NLRP3 inflammasome is in line with a recent report that FXR protects against cholestasis-associated sepsis through its interaction with NLRP3 and CASP1 in macrophages (Hao et al., 2017). Our findings advance our understanding of the inhibitory effect of FXR on inflammasome gene regulation in hepatocytes subjected to ER stress. Moreover, the finding that FXR is upregulated in NAFLD human samples in the absence of inflammasome activation indicates that pathological events can also adaptively stimulate FXR expression in the liver during disease progression. So this inhibitory effect of FXR on inflammasome gene regulation might vary depending on disease severity. For example, most NAFLD patients in our study had mild to moderate steatosis (i.e., grade 1 or 2), which might account for the lack of IL-1 β increase, as previously reported (Csak et al., 2011). Consequently, FXR levels might be repressed in certain conditions or adaptively enhanced in others. Thus, FXR might be an attractive target to inhibit the priming and activation processes of inflammasome and inflammasome-mediated liver diseases.

Hepatocytes make up 70%–85% of the liver mass, have high metabolic activity, and have an abundance of ER, allowing this cell type to serve as a major sensor responding to ER stress. The ER stress-activated NLRP3 inflammasome may lead to hepatocyte injury. Consistent with our results, FXR was shown to be decreased upon ER stress (Xiong et al., 2014), suggestive of a feedforward loop between FXR loss and ER stress. An important finding of our study is the identification of FXR as a hepatoprotective regulator against catastrophic ER stress; our findings show that FXR ligand treatment ameliorated ER stress-mediated hepatocyte death and liver injury. Because mitochondrial function is closely linked to ER stress and inflammasome activation (Gurung et al., 2015; Senft and Ronai, 2015), the beneficial effects of FXR on energy metabolism and mitochondrial function (Lee et al., 2012; Teodoro et al., 2011) may add value to the use of FXR as a therapeutic target for ER stress-associated liver diseases.

NLRP3 gene regulation is poorly understood. Here, we identified PERK as a pathway for NLRP3 induction. In our siRNA experiments, we knocked down components of three canonical UPR pathways and revealed that PERK signaling is specifically involved in NLRP3 induction by ER stress in hepatocytes. In support of this, NLRP3 expression was enhanced by PERK overexpression, and IL-1 β production was attenuated by *Perk* knockdown. In addition, our results show that FXR modulates PERK phosphorylation and subsequent CHOP expression. Our findings indicate that CHOP is a potential transcriptional factor that is necessary for NLRP3 expression downstream of PERK, and the ChIP assay results confirm that CHOP interacts with the *NLRP3* gene. Of the three CHOP response elements located

within the –2.2-kb promoter region of the human *NLRP3* gene, the core sequences of CHOP-RE1 and CHOP-RE3 resemble CCAAT-enhancer binding protein-activating transcription factor (C/EBP-ATF) response elements (CAREs) (Kilberg et al., 2009; Teske et al., 2013). Additionally, the same CHOP-RE2 sequence regulated TRB3, another ER stress-inducible gene (Ohoka et al., 2005). CHOP promotes cell death signals through the regulation of pro-CASP1 (Lebeaupin et al., 2015). Therefore, the identified PERK-CHOP pathway seems to be critical for inflammasome-mediated hepatocyte death during the progression of liver diseases.

TXNIP interacts with various proteins, including NLRP3 (Yoshihara et al., 2014; Zhou et al., 2010). Emerging evidence suggests that TXNIP plays a role in ER stress-mediated cell death and in the NLRP3 inflammasome activation step (Abderrazak et al., 2015; Lerner et al., 2012; Osowski et al., 2012; Zhou et al., 2010). Our results demonstrate that *Fxr* KO mice displayed robust changes in TXNIP levels and severe liver injury in response to ER stress. Consistently, FXR activation attenuated the ER stress-mediated induction of TXNIP. Thus, the ability of FXR to inhibit TXNIP may contribute to the inhibition of the NLRP3 inflammasome. We also showed that ER stress induced TXNIP through the PERK-CHOP pathway in hepatocytes. However, TXNIP seemed to not be directly regulated by CHOP, as suggested by the lack of CHOP binding sites within the –5-kb human *TXNIP* promoter region. TXNIP belongs to the ATF5-specific genes (Teske et al., 2013). So, CHOP may indirectly control TXNIP through ATF5 (Teske et al., 2013). In contrast to NLRP3, TXNIP was also affected by IRE1 pathway in hepatocytes, which is consistent with the finding that IRE1 destabilized miR-17 for TXNIP in pancreatic beta cells (Lerner et al., 2012). These findings indicate that NLRP3 and TXNIP expression might be differentially controlled by UPR signaling. TXNIP serves as an inhibitory partner of thioredoxin, regulating redox homeostasis in cells (Lu and Holmgren, 2014; Yoshihara et al., 2014). Thus, the overexpression of NLRP3 and its binding partner TXNIP might contribute to ER stress-induced hepatocyte injury and be augmented by FXR deficiency.

NCK1 is the SRC homology domain-containing adaptor protein, functionally linking cell surface receptors with the actin cytoskeleton (Li et al., 2001). NCK1 interacts with PERK through protein-protein binding, inhibiting the activity of PERK (Yamani et al., 2014, 2015). In this study, we proposed that NCK1 has a functional role in the FXR regulation of the UPR pathway in hepatocytes (i.e., that FXR inhibits PERK through NCK1 expression). Our data show that ER stress inhibited NCK1 and that this effect was overcome by FXR activation. Moreover, our results show that the siRNA-mediated knockdown of *Nck1* attenuated the inhibitory effects of FXR on NLRP3, TXNIP, and CHOP expression under ER stress condition. Consistently, the rescuing effect of FXR agonist on cell viability was diminished by *Nck1* silencing.

(G) qRT-PCR assays for *Nlrp3* in AML12 cells transfected with Mock or *Perk*-overexpressing vector for 24 hr. Immunoblots confirmed *Perk* overexpression (O/E). Data represent the mean \pm SEM of three separate experiments.

(H) ELISA for mature IL-1 β . Assays were done on the media prepared from AML12 cells treated as in (B). Data represent the mean \pm SEM (N = 3 each).

For (A)–(E), relative protein levels were assessed by scanning densitometry of the immunoblots and normalized to those of β -actin. See also Figure S2. In (E)–(H), *p < 0.05, **p < 0.01.

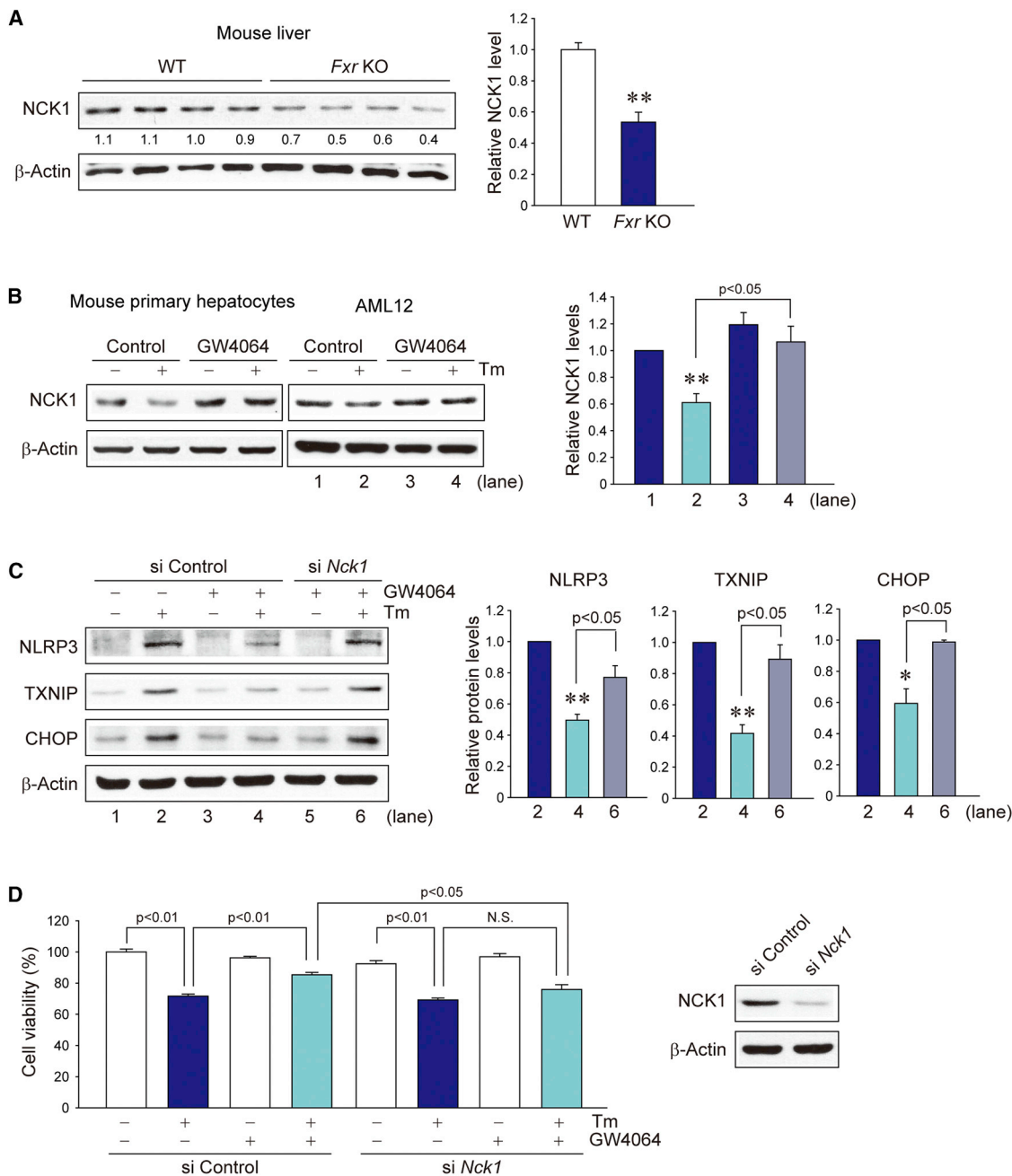


Figure 6. NCK1 Is Involved in FXR Effect on NLRP3 Inflammasome

(A) Immunoblot of NCK1 in wild-type (WT) and *Fxr* KO mouse liver. Data represent the mean \pm SEM (N = 4 each).

(B) Immunoblots of NCK1 in hepatocytes. Cells were treated as described in Figure 3C. Data represent the mean \pm SEM of three separate experiments.

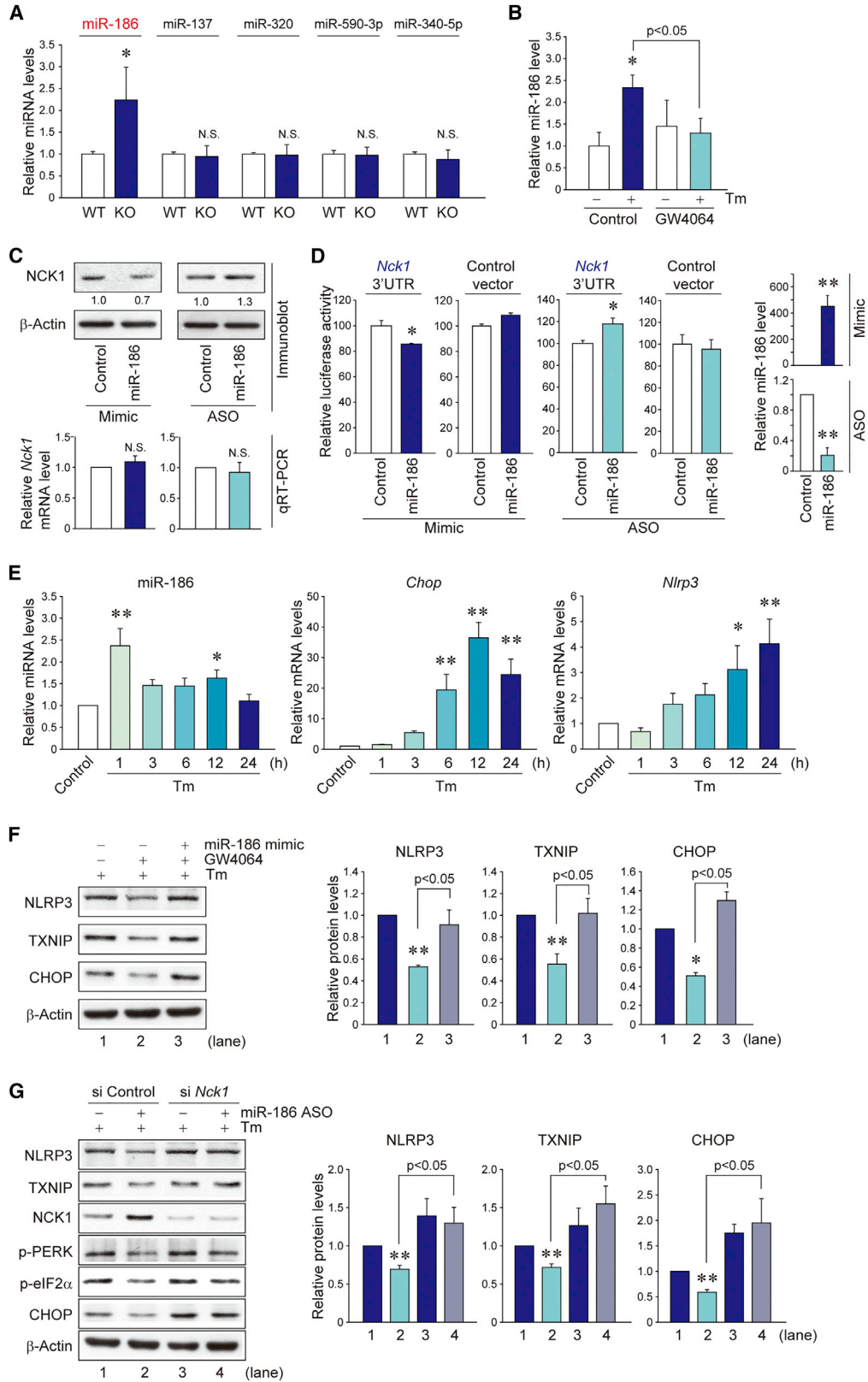
(C) Immunoblots for NLRP3, TXNIP, and CHOP. After transfection with control siRNA or *Nck1* siRNA for 48 hr, AML12 cells were pre-treated with GW4064 for 1 hr and continuously exposed to Tm for 24 hr. Data represent the mean \pm SEM of three separate experiments.

(D) 3-(4,5-dimethylthiazol-2-yl)-2,5-diphenyl-tetrazolium bromide (MTT) assays after *Nck1* knockdown. AML12 cells were similarly treated as in (C) (Tm; 48 hr). Immunoblotting confirmed the knockdown effect. Data represent the mean \pm SEM (N = 5 each).

For (A)–(C), relative protein levels were assessed by scanning densitometry of the immunoblots and normalized to those of β -actin. *p < 0.05, **p < 0.01.

Thus, the inhibition of the NLRP3 inflammasome by FXR, and the consequent attenuation of hepatocyte injury in response to ER stress, may depend on NCK1, indicating that a rheostatic balance might exist between NCK1 and PERK.

miR-186 has been studied in the field of cancer biology (Cai et al., 2013; Ruan et al., 2016; Zhu et al., 2016). Here, we report a role for miR-186 in the regulation of ER stress-induced NLRP3 inflammasome activation. Of the putative microRNAs targeting



(legend on next page)

NCK1, FXR specifically regulated miR-186 in our study. Consistently, the ligand-mediated activation of FXR prevented ER stress from causing an increase in miR-186 levels. Our results indicate that miR-186 might inhibit NCK1, as supported by the experiments where we used a miR-186 mimic or inhibitor (ASO). In these experiments, transfecting hepatocyte cell models with a miR-186 mimic prevented NLRP3 inflammasome downregulation by FXR under ER stress condition. By the same token, the knocking down of *Nck1* reversed the inhibitory effect of miR-186 ASO on the NLRP3 inflammasome, indicating that a functional association might exist between these molecules and NLRP3 inflammasome activation in hepatocytes. Our time course study also verified that a temporal relationship exists between the expression of miR-186, CHOP, and NLRP3. In our supplementary analysis, a p53 binding site was predicted in the promoter region of miR-186. Hence, we do not exclude the possibility that small heterodimer partner-mediated p53 inhibition (Lee et al., 2010) contributes to the regulation of miR-186.

Overall, our results demonstrate that FXR acts as a regulator of hepatic ER stress and of NLRP3 inflammasome activation through the PERK-CHOP signaling pathway and support the hypothesis that FXR regulation of miR-186/NCK1 may contribute to the inhibition of ER stress. Our findings provide key information on targets for liver diseases that feature ER stress-mediated inflammasome and indicate that the ligand-based activation of FXR might provide a therapeutic approach to overcoming ER stress-mediated liver disease progression.

EXPERIMENTAL PROCEDURES

Information on the materials used in this study and the details of how the *in vivo* and *in vitro* assays were performed are provided in [Supplemental Information](#).

Patient Samples

We used liver samples from patients with NAFLD (or NASH) that were reported in a previous study (Ahn et al., 2014). The clinical characteristics of these patients, the control groups used, and the criteria used to exclude patients from the study are explained in Ahn et al. (2014). All control individuals had <5% hepatic fat content and normal liver enzymes. The study was approved by the Institutional Review Boards at Eulji Hospital or Hanyang University Hospital. The protocol was registered at the Clinical Research Information Service with the registration number KCT0000900 (<http://cris.nih.go.kr/cris/index.jsp>). Histological assessment of liver biopsy

samples (i.e., NAFLD activity score) and the interpretation of immunohistochemical stains (i.e., H-score assignment) were performed as described in Ahn et al. (2014).

Animal Treatment

Animal experiments were conducted under the guidelines of the Institutional Animal Care and Use Committee at Seoul National University. C57BL/6 mice were purchased from Charles River Orient (Seoul, Korea). *Fxr* KO mice were obtained from the Jackson Laboratory. The animals were housed at 20°C ± 2°C with 12 hr light/dark cycles and a relative humidity of 50% ± 5% under filtered, pathogen-free air, with food and water available *ad libitum*. For animal models of liver injury, 8-week-old male C57BL/6 mice were injected intraperitoneally (i.p.) with a single dose of vehicle or with APAP (500 mg/kg body weight) for 6 hr. In a separate experiment, 8-week-old male C57BL/6 mice were treated with vehicle or with CCl₄ (0.6 mL/kg body weight, i.p., twice a week) for 6 weeks. For the NASH animal model, 3-week-old C57BL/6 male mice were fed with a MCDHF diet or with a sterile standard control diet for 6 weeks (Park et al., 2016). To induce ER stress, wild-type or *Fxr* KO mice (8 weeks old, male) were injected (i.p.) with a single dose of vehicle or with Tm (2 mg/kg) and were sacrificed 2 days after injection. An animal model of FXR activation was achieved by injecting wild-type (8 weeks old, male) mice with vehicle or with GW4064 (30 mg/kg, i.p.) twice at an interval of 12 hr. One hour after the second GW4064 treatment, mice were injected (i.p.) with a single dose of Tm and sacrificed 3 days later. Blood and liver samples were taken for serum biochemical and histopathological analyses in all animal experiments.

RNA Isolation and Real-Time RT-PCR Assays

Total RNA was extracted with TRIzol (Invitrogen, Carlsbad, CA) and was reverse transcribed to obtain cDNA. qRT-PCR was done according to the manufacturer's instructions using a StepOne real-time PCR instrument (Thermo Fisher Scientific) and SYBR Premix Ex TaqII kit (Takara Bio, Shiga, Japan).

Cell Culture

The cell lines, AML12 (mouse hepatocyte-derived cell line) and HepG2 (human hepatocyte-derived cell line), were purchased from ATCC (Rockville, MD, USA). The isolation of primary hepatocytes from mice is described in the [Supplemental Experimental Procedures](#).

Statistical Analysis

Statistically significant differences were assessed by the Student's t test or by one-way ANOVA tests. For each statistically significant effect of treatment, the Bonferroni's or least significant difference (LSD) methods were used for comparisons between multiple group means. The data were expressed as mean ± SEM. The criterion for statistical significance was set at $p < 0.05$ or $p < 0.01$. Statistical analyses were performed using IBM SPSS Statistics 23 software.

Figure 7. miR-186 Contributes to ER Stress-Induced NLRP3 Inflammasome Activation

(A and B) qRT-PCR assays for the miRNAs that putatively target NCK1 in mouse liver (A). miR-186 levels were additionally measured in mice treated as described in Figure 3B (B). Data represent the mean ± SEM (N = 3 or 6 for each treatment). Statistical significance of differences between *Fxr* KO and wild-type (WT) group (* $p < 0.05$), or each treatment and control group (* $p < 0.05$), was determined (N.S., not significant).

(C) Immunoblots (upper) or qRT-PCR assays (lower) for NCK1 in AML12 cells transfected with miR-186 mimic (or control) or miR-186 ASO (or control) for 48 hr. Data represent the mean ± SEM of three separate experiments.

(D) *Nck1* 3' UTR reporter activity. Luciferase activity was measured in HepG2 cells transfected with miR-186 mimic or miR-186 ASO in combination with a luciferase reporter comprising *Nck1* 3' UTR. The specificity of miR-186 mimic or ASO action was confirmed by the use of control vector (left). qRT-PCR assays verified overexpression or silencing of miR-186 (right). Data represent the mean ± SEM (N = 3 or 6 each).

(E) qRT-PCR assays for miR-186, *Chop*, and *Nlrp3* in AML12 cells treated with Tm for indicated times. Data represent the mean ± SEM of three separate experiments.

(F) Immunoblots for NLRP3, TXNIP, and CHOP. After transfection with control mimic or miR-186 mimic for 48 hr, AML12 cells were pre-treated with GW4064 for 1 hr and continuously exposed to Tm for 24 hr.

(G) Immunoblots of the proteins of interest. AML12 cells were treated with Tm for 24 hr after transfection with miR-186 ASO (or control ASO) and/or *Nck1* siRNA (or control siRNA) for 48 hr.

For (F) and (G), relative protein levels were assessed by scanning densitometry of the immunoblots and normalized to those of β -actin. Data represent the mean ± SEM of three separate experiments. In (D)–(G), * $p < 0.05$, ** $p < 0.01$.

DATA AND SOFTWARE AVAILABILITY

Original data have been deposited to Mendeleev Data and are available at <https://doi.org/10.17632/rj74h4tp3f.1>.

SUPPLEMENTAL INFORMATION

Supplemental Information includes Supplemental Experimental Procedures and two figures and can be found with this article online at <https://doi.org/10.1016/j.celrep.2018.07.068>.

ACKNOWLEDGMENTS

This research was supported by the National Research Foundation of Korea (NRF) grant funded by the Korea government (Ministry of Science and ICT [MSIP]; NRF-2015R1A2A1A10052663) for S.G.K. and the Basic Science Research Program through NRF funded by the Ministry of Education (2017R1D1A1B03028272) for C.Y.H. The authors thank Dr. Bart Staels (Institut Pasteur de Lille, Lille, France) for providing FXRE luciferase reporter.

AUTHOR CONTRIBUTIONS

Study Concept and Design, C.Y.H., H.S.R., and S.G.K.; Acquisition of Data, C.Y.H., H.S.R., A.K., K.J., and D.W.J.; Analysis and Interpretation of Data, C.Y.H., H.S.R., A.K., K.J., D.W.J., and S.G.K.; Statistical Analysis, C.Y.H. and H.S.R.; Drafting of the Manuscript, C.Y.H. and H.S.R.; Obtained Funding, C.Y.H. and S.G.K.; Administrative, Technical, and Material Support, T.H.K., J.W.K., and B.K.; Critical Revision of the Manuscript for Important Intellectual Content, S.G.K.; Study Supervision, S.G.K.

DECLARATION OF INTERESTS

The authors declare no competing interests.

Received: April 18, 2018

Revised: July 10, 2018

Accepted: July 18, 2018

Published: September 11, 2018

REFERENCES

- Abderrazak, A., Syrovets, T., Couchie, D., El Hadri, K., Friguet, B., Simmet, T., and Rouis, M. (2015). NLRP3 inflammasome: from a danger signal sensor to a regulatory node of oxidative stress and inflammatory diseases. *Redox Biol.* *4*, 296–307.
- Adorini, L., Pruzanski, M., and Shapiro, D. (2012). Farnesoid X receptor targeting to treat nonalcoholic steatohepatitis. *Drug Discov. Today* *17*, 988–997.
- Ahn, S.B., Jang, K., Jun, D.W., Lee, B.H., and Shin, K.J. (2014). Expression of liver X receptor correlates with intrahepatic inflammation and fibrosis in patients with nonalcoholic fatty liver disease. *Dig. Dis. Sci.* *59*, 2975–2982.
- Beuers, U., Trauner, M., Jansen, P., and Poupon, R. (2015). New paradigms in the treatment of hepatic cholestasis: from UDCA to FXR, PXR and beyond. *J. Hepatol.* *62* (1, Suppl), S25–S37.
- Cai, J., Wu, J., Zhang, H., Fang, L., Huang, Y., Yang, Y., Zhu, X., Li, R., and Li, M. (2013). miR-186 downregulation correlates with poor survival in lung adenocarcinoma, where it interferes with cell-cycle regulation. *Cancer Res.* *73*, 756–766.
- Calkin, A.C., and Tontonoz, P. (2012). Transcriptional integration of metabolism by the nuclear sterol-activated receptors LXR and FXR. *Nat. Rev. Mol. Cell Biol.* *13*, 213–224.
- Carr, R.M., and Reid, A.E. (2015). FXR agonists as therapeutic agents for non-alcoholic fatty liver disease. *Curr. Atheroscler. Rep.* *17*, 500.
- Csak, T., Ganz, M., Pespisa, J., Kodyas, K., Dolganiuc, A., and Szabo, G. (2011). Fatty acid and endotoxin activate inflammasomes in mouse hepatocytes that release danger signals to stimulate immune cells. *Hepatology* *54*, 133–144.
- Dara, L., Ji, C., and Kaplowitz, N. (2011). The contribution of endoplasmic reticulum stress to liver diseases. *Hepatology* *53*, 1752–1763.
- Guo, H., Callaway, J.B., and Ting, J.P. (2015). Inflammasomes: mechanism of action, role in disease, and therapeutics. *Nat. Med.* *21*, 677–687.
- Gurung, P., Lukens, J.R., and Kanneganti, T.D. (2015). Mitochondria: diversity in the regulation of the NLRP3 inflammasome. *Trends Mol. Med.* *21*, 193–201.
- Han, C.Y., Lim, S.W., Koo, J.H., Kim, W., and Kim, S.G. (2016). PHLDA3 overexpression in hepatocytes by endoplasmic reticulum stress via IRE1-Xbp1s pathway expedites liver injury. *Gut* *65*, 1377–1388.
- Hao, H., Cao, L., Jiang, C., Che, Y., Zhang, S., Takahashi, S., Wang, G., and Gonzalez, F.J. (2017). Farnesoid X receptor regulation of the NLRP3 inflammasome underlies cholestasis-associated sepsis. *Cell Metab.* *25*, 856–867.e5.
- Hetz, C. (2012). The unfolded protein response: controlling cell fate decisions under ER stress and beyond. *Nat. Rev. Mol. Cell Biol.* *13*, 89–102.
- Kilberg, M.S., Shan, J., and Su, N. (2009). ATF4-dependent transcription mediates signaling of amino acid limitation. *Trends Endocrinol. Metab.* *20*, 436–443.
- Latreille, M., and Larose, L. (2006). Nck in a complex containing the catalytic subunit of protein phosphatase 1 regulates eukaryotic initiation factor 2alpha signaling and cell survival to endoplasmic reticulum stress. *J. Biol. Chem.* *281*, 26633–26644.
- Lebeaupin, C., Proics, E., de Bieville, C.H., Rousseau, D., Bonnafous, S., Pataouraux, S., Adam, G., Lavallard, V.J., Rovere, C., Le Thuc, O., et al. (2015). ER stress induces NLRP3 inflammasome activation and hepatocyte death. *Cell Death Dis.* *6*, e1879.
- Lee, J., Padhye, A., Sharma, A., Song, G., Miao, J., Mo, Y.Y., Wang, L., and Kemper, J.K. (2010). A pathway involving farnesoid X receptor and small heterodimer partner positively regulates hepatic sirutin 1 levels via microRNA-34a inhibition. *J. Biol. Chem.* *285*, 12604–12611.
- Lee, C.G., Kim, Y.W., Kim, E.H., Meng, Z., Huang, W., Hwang, S.J., and Kim, S.G. (2012). Farnesoid X receptor protects hepatocytes from injury by repressing miR-199a-3p, which increases levels of LKB1. *Gastroenterology* *142*, 1206–1217.e7.
- Lerner, A.G., Upton, J.P., Praveen, P.V., Ghosh, R., Nakagawa, Y., Igbaria, A., Shen, S., Nguyen, V., Backes, B.J., Heiman, M., et al. (2012). IRE1 α induces thioredoxin-interacting protein to activate the NLRP3 inflammasome and promote programmed cell death under irremediable ER stress. *Cell Metab.* *16*, 250–264.
- Li, W., Fan, J., and Woodley, D.T. (2001). Nck/Dock: an adapter between cell surface receptors and the actin cytoskeleton. *Oncogene* *20*, 6403–6417.
- Lu, J., and Holmgren, A. (2014). The thioredoxin antioxidant system. *Free Radic. Biol. Med.* *66*, 75–87.
- Malhi, H., and Kaufman, R.J. (2011). Endoplasmic reticulum stress in liver disease. *J. Hepatol.* *54*, 795–809.
- Maloney, P.R., Parks, D.J., Haffner, C.D., Fivush, A.M., Chandra, G., Plunket, K.D., Creech, K.L., Moore, L.B., Wilson, J.G., Lewis, M.C., et al. (2000). Identification of a chemical tool for the orphan nuclear receptor FXR. *J. Med. Chem.* *43*, 2971–2974.
- Nissim, O., Melis, M., Diaz, G., Kleiner, D.E., Tice, A., Fantola, G., Zamboni, F., Mishra, L., and Farci, P. (2012). Liver regeneration signature in hepatitis B virus (HBV)-associated acute liver failure identified by gene expression profiling. *PLoS ONE* *7*, e49611.
- Ohoka, N., Yoshii, S., Hattori, T., Onozaki, K., and Hayashi, H. (2005). TRB3, a novel ER stress-inducible gene, is induced via ATF4-CHOP pathway and is involved in cell death. *EMBO J.* *24*, 1243–1255.
- Oslowski, C.M., Hara, T., O'Sullivan-Murphy, B., Kanekura, K., Lu, S., Hara, M., Ishigaki, S., Zhu, L.J., Hayashi, E., Hui, S.T., et al. (2012). Thioredoxin-interacting protein mediates ER stress-induced β cell death through initiation of the inflammasome. *Cell Metab.* *16*, 265–273.
- Park, S., Kim, J.W., Yun, H., Choi, S.J., Lee, S.H., Choi, K.C., Lim, C.W., Lee, K., and Kim, B. (2016). Mainstream cigarette smoke accelerates the progression of nonalcoholic steatohepatitis by modulating Kupffer cell-mediated hepatocellular apoptosis in adolescent mice. *Toxicol. Lett.* *256*, 53–63.

- Ruan, T., He, X., Yu, J., and Hang, Z. (2016). MicroRNA-186 targets Yes-associated protein 1 to inhibit Hippo signaling and tumorigenesis in hepatocellular carcinoma. *Oncol. Lett.* *11*, 2941–2945.
- Senft, D., and Ronai, Z.A. (2015). UPR, autophagy, and mitochondria crosstalk underlies the ER stress response. *Trends Biochem. Sci.* *40*, 141–148.
- Szabo, G., and Csak, T. (2012). Inflammasomes in liver diseases. *J. Hepatol.* *57*, 642–654.
- Szabo, G., and Petrasek, J. (2015). Inflammasome activation and function in liver disease. *Nat. Rev. Gastroenterol. Hepatol.* *12*, 387–400.
- Teodoro, J.S., Rolo, A.P., and Palmeira, C.M. (2011). Hepatic FXR: key regulator of whole-body energy metabolism. *Trends Endocrinol. Metab.* *22*, 458–466.
- Teske, B.F., Fusakio, M.E., Zhou, D., Shan, J., McClintick, J.N., Kilberg, M.S., and Wek, R.C. (2013). CHOP induces activating transcription factor 5 (ATF5) to trigger apoptosis in response to perturbations in protein homeostasis. *Mol. Biol. Cell* *24*, 2477–2490.
- Wan, X., Xu, C., Lin, Y., Lu, C., Li, D., Sang, J., He, H., Liu, X., Li, Y., and Yu, C. (2016). Uric acid regulates hepatic steatosis and insulin resistance through the NLRP3 inflammasome-dependent mechanism. *J. Hepatol.* *64*, 925–932.
- Wang, Y.D., Chen, W.D., Moore, D.D., and Huang, W. (2008). FXR: a metabolic regulator and cell protector. *Cell Res.* *18*, 1087–1095.
- Wree, A., Eguchi, A., McGeough, M.D., Pena, C.A., Johnson, C.D., Canbay, A., Hoffman, H.M., and Feldstein, A.E. (2014). NLRP3 inflammasome activation results in hepatocyte pyroptosis, liver inflammation, and fibrosis in mice. *Hepatology* *59*, 898–910.
- Xiong, X., Wang, X., Lu, Y., Wang, E., Zhang, Z., Yang, J., Zhang, H., and Li, X. (2014). Hepatic steatosis exacerbated by endoplasmic reticulum stress-mediated downregulation of FXR in aging mice. *J. Hepatol.* *60*, 847–854.
- Yamani, L., Latreille, M., and Larose, L. (2014). Interaction of Nck1 and PERK phosphorylated at Y⁵⁶¹ negatively modulates PERK activity and PERK regulation of pancreatic β -cell proinsulin content. *Mol. Biol. Cell* *25*, 702–711.
- Yamani, L., Li, B., and Larose, L. (2015). Nck1 deficiency improves pancreatic β cell survival to diabetes-relevant stresses by modulating PERK activation and signaling. *Cell. Signal.* *27*, 2555–2567.
- Yoshihara, E., Masaki, S., Matsuo, Y., Chen, Z., Tian, H., and Yodoi, J. (2014). Thioredoxin/Txnip: redoxosome, as a redox switch for the pathogenesis of diseases. *Front. Immunol.* *4*, 514.
- Zhou, R., Tardivel, A., Thorens, B., Choi, I., and Tschopp, J. (2010). Thioredoxin-interacting protein links oxidative stress to inflammasome activation. *Nat. Immunol.* *11*, 136–140.
- Zhu, X., Shen, H., Yin, X., Long, L., Xie, C., Liu, Y., Hui, L., Lin, X., Fang, Y., Cao, Y., et al. (2016). miR-186 regulation of Twist1 and ovarian cancer sensitivity to cisplatin. *Oncogene* *35*, 323–332.